Attosecond-scale absorption at extreme intensities

A. F. Savin,[1] A. J. Ross,[1] M. Serzans,[1] R. M. G. M. Trines,[2] L. Ceurvorst,[1] N. Ratan,[1] B. Spiers,[1] R. Bingham,[2,3] A. P. L. Robinson,[2] and P. A. Norreys[1,2]
[1]*Clarendon Laboratory, University of Oxford, Oxford OX1 3PU, United Kingdom*
[2]*Central Laser Facility, STFC Rutherford Appleton Laboratory, Didcot, Oxon OX11 0QX, United Kingdom*
[3]*Department of Physics, SUPA, University of Strathclyde, Glasgow, Scotland G4 ONG, United Kingdom*

(Received 12 June 2017; accepted 22 October 2017; published online 8 November 2017)

A novel non-ponderomotive absorption mechanism, originally presented by Baeva *et al.* [Phys. Plasmas **18**, 056702 (2011)] in one dimension, is extended into higher dimensions for the first time. This absorption mechanism, the Zero Vector Potential (ZVP), is expected to dominate the interactions of ultra-intense laser pulses with critically over-dense plasmas such as those that are expected with the Extreme Light Infrastructure laser systems. It is shown that the mathematical form of the ZVP mechanism and its key scaling relations found by Baeva *et al.* in 1D are identically reproduced in higher dimensions. The two dimensional particle-in-cell simulations are then used to validate both the qualitative and quantitative predictions of the theory. https://doi.org/10.1063/1.4989798

I. INTRODUCTION

The completion and commissioning in the near future of multi-PW laser systems (particularly those in the Czech Republic, Hungary, and Romania via the Extreme Light Infrastructure project[1] and the Apollon laser in France[2]) will soon allow a wealth of new physics to be studied for the first time. New physics at the intensity frontier includes the onset of pair production via non-linear QED processes;[3] multi-GeV acceleration of electron bunches in laser wakefield accelerators;[4] ion beam characterisation via radiation pressure acceleration,[5] channel formation, and hole-boring,[6,7] and coherent harmonic generation and focusing,[8] among many others.

All of these topics benefit from a fundamental understanding of the energy absorption processes that occur under extreme intensities. In this paper, we build on the work of Baeva *et al.*,[9] extending the theory of the Zero Vector Potential (ZVP) absorption mechanism from one to three dimensions for the first time. The interaction is shown to be an essentially planar effect via the analytic theory with the principal dynamics of the interaction confined to the plane formed by the directions of polarisation and propagation of the laser pulse's vector potential. This is followed by a numerical validation of the theory to be conducted using the two dimensional (2D) particle-in-cell (PIC) simulations.

The results from the simulations are then presented, extending the results of Baeva *et al.*'s one dimensional (1D) numerical work. We show that, as in the 1D case, the electrons absorb the laser energy and form high momentum bunches that co-propagate with zeroes in the vector potential of the laser pulse that are penetrating the skin layer of the plasma, where the vector potential is taken in the Lorenz gauge and can therefore be defined as[10]

$$\vec{A}(\vec{r},t) = \frac{\mu_0}{4\pi}\int \frac{\vec{J}(\vec{r'},t')}{|\vec{r}-\vec{r'}|}d^3\vec{r'}, \tag{1}$$

where $t' = t - |\vec{r}-\vec{r'}|/c$ is the "retarded time" of the system caused by the finite speed of transmission of light. It is also found that due to the coherent nature of the interaction, the ZVP mechanism increases the efficiency of High Harmonic Generation (HHG). In this way, the ZVP mechanism allows the understanding of HHG to move away from approximations[11] and towards a more complete description of the intense laser-plasma interactions.

The short duration—on the scale of attoseconds—of these electron bunches and the subsequently generated coherent x-rays opens up new avenues for diagnostics and the exploration of fundamental science. Attosecond pulses are of great import to many areas such as the temporally resolved measurements of chemical bonds, bio-information, diagnosis of microchip transistors, resolving the details of molecular destruction in destructive scattering experiments,[12–14] and most recently probing the water window.[15]

The outline of the paper is as follows: in Sec. II, we describe the conditions necessary for the ZVP mechanism to contribute significantly to absorption. We then explain the mechanics of the process via the reconstruction of the electron skin layer in Sec. III. The manner in which the electron energy scales with the initial conditions of the system is given an exposition in Sec. IV. Finally, these scaling relations, as well as the quantitative predictions of Sec. III are tested using 2D PIC simulations, the results of which are presented in Sec. V. Future applications that will benefit from this new understanding, such as coherent attosecond X-ray harmonic generation and focusing, concludes the paper.

II. ZERO VECTOR POTENTIAL REGIME

A variety of theories are used to describe the absorption of laser energy by a plasma across a range of regimes.[16] The examples include the ponderomotive mechanism,[17] Brunel heating,[18] harmonic and anharmonic resonant absorption,[19,20]

and vacuum heating.[21] However, in the limit of ultra-intense laser pulses and critically over-dense plasmas, non-ponderomotive mechanisms such as the ZVP mechanism could begin to contribute significantly to absorption. This regime, which is expected to be easily accessible and scanned by the Extreme Light Infrastrucutre[1] is characterised by the two dimensionless parameters a_0 and S being greater than unity. a_0 is the normalised vector potential[11] given by

$$a_0 = \frac{eA}{m_e c}, \tag{2}$$

where A is the vector potential of the laser pulse. S is the relativistic similarity parameter[22] given by

$$S = \frac{n_e}{a_0 n_c}, \tag{3}$$

where n_e is the number density of the electrons in the plasma and n_c is the critical density[23] above which a material is opaque to light of angular frequency ω_0

$$n_c = \frac{m_e \epsilon_0}{e^2}\omega_0^2. \tag{4}$$

In this regime, Baeva *et al.* showed that the electron plasma frequency, $\omega_p = \sqrt{n_e e^2/m_e\epsilon_0}$, is so high that the electrons are able to respond adiabatically to the ponderomotive $\vec{j}\times\vec{B}$-force, which oscillates at a frequency $2\omega_0$. The effect of this is to displace the electrons in the skin layer of the plasma from the ion background leaving behind a positive space charge. The electrons then find themselves confined within a potential well that has been set up by a balance between the ponderomotive pressure and the electrostatic Coulomb force. What follows now is an extension of the theoretical work presented by Baeva *et al.* into three dimensions, including the case of oblique incidence and a subsequent extension of the numerical work using 2D PIC simulations.

III. ABSORPTION VIA RECONSTRUCTION OF THE SKIN LAYER

To grasp the workings of the ZVP absorption mechanism, it is necessary to investigate the nature of the potential well mentioned at the end of Sec. II. An electron inside this potential well can be described by the Hamiltonian[9]

$$\mathcal{H} = c\sqrt{|\vec{p}|^2 + m_e^2 c^2} + \Phi, \tag{5}$$

where the first term in the Hamiltonian is a simple extraction of the energy from the invariant of the relativistic 4-momentum ($P^\mu = (E/c, \vec{p})$, $P^\mu \cdot P_\mu = m^2c^2$) in the Minkowski metric.[24] Φ is a spatial electrostatic potential energy contribution from the fields in the plasma, and so is zero outside of the plasma. What follows in this section is a step by step path through the equations governing the ZVP mechanism resulting in Eqs. (8) and (14): the two key results of Baeva *et al.*,[9] but this time in the more general case of a 3D system.

By conserving momentum along the direction of the polarisation of the vector potential, it is easily determined that $\vec{p}_{\text{pol}} = e\vec{A}$. Therefore, the Hamiltonian in Eq. (5) can be modified to

$$\mathcal{H} = c\left[p_{\text{prop}}^2 + p_\perp^2 + e^2A^2 + m_e^2c^2\right]^{1/2} + \Phi, \tag{6}$$

where p_{prop} is the electron momentum in the direction of the propagation of the laser pulse, and $p_\perp$ is the electron momentum in the direction mutually perpendicular with the directions of propagation and polarisation.

Equation (6) shows that should the vector potential pass through zero then the potential well will be disrupted and the adiabatic state of the electrons will be broken. To proceed further with this hypothesis, consider the case of a Gaussian pulse incident upon a plasma expanding in the negative $\hat{y}$-direction at a speed u. The direction of propagation of the pulse can, without loss of generality, be confined to the x-y plane at a general angle, θ, to the y-axis and a general angle of polarisation, φ, to the x-y plane. Such a scenario is displayed in Fig. 1. In the rest frame of the expanding plasma (hereafter referred to simply as "the rest frame" and denoted as the primed frame in the following notation), the vector potential of a Gaussian laser pulse can be described as

$$\vec{A}'(r,l,t) = A_0\hat{P}\frac{w_0}{w(l)}\exp\left[-\left(\frac{r^2}{w(l)^2} + \frac{t^2}{\tau^2} + \frac{l}{\delta_S}\right)\right] \times\cos\left[\omega t - k\left(l + \frac{r^2}{2R(l)}\right) + \psi(l)\right], \tag{7}$$

where l is the distance along the axis of propagation from focus, r is the perpendicular distance from said axis, $\hat{P} = (\cos\varphi\cos\theta,\ \cos\varphi\sin\theta,\ \sin\varphi)$ is the unit vector in the direction of the polarisation of the laser pulse, w_0 is the beam waist of the pulse at focus, $w(l) = \sqrt{1 + (l/z_R)^2}$ is the beam waist of the pulse away from focus, τ is the duration of the pulse, $R(l) = l[1 + (z_R/l)^2]$ is the radius of curvature of the beam, $\psi(l) = \arctan(l/z_R)$ is the Gouy phase of the pulse, and $z_R = kw_0^2/2$ is the Rayleigh range of the pulse.[25]

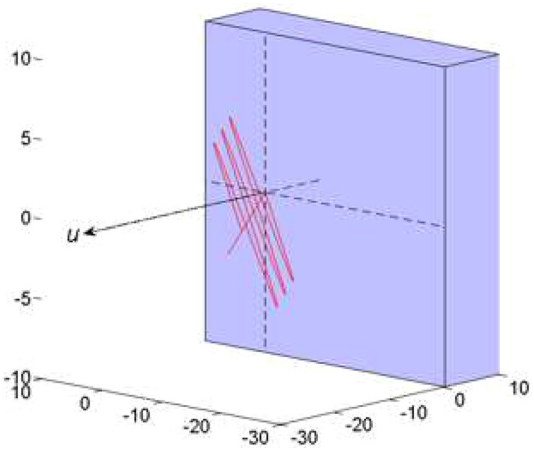

FIG. 1. A simple schematic displaying the scenario under consideration for the ZVP mechanism. A laser pulse is obliquely incident upon a plasma expanding with a typical speed, u.

Within the geometry shown in Fig. 1, the distances r and l can be expressed as $r^2 = (x'\cos\theta + y'\sin\theta)^2 + z'^2$ and $l^2 = x'^2 + y'^2 - r^2$, respectively. A simple Doppler shift into the laboratory frame, expressed by $x' = x$, $z' = z$, and $y' = y + ut$ yields the functional form of the vector potential in the laboratory frame

$$\vec{A}(x,y,z,t) = \vec{S}(x,y,z,t)\cos\left[f(x,y,z,t)\right], \tag{8}$$

where $\vec{S}(x,y,z,t)$ contains all of the information about the polarisation, magnitude, and exponential decay inside the skin layer of the pulse.

The function $f(x, y, x, t)$ in Eq. (8), can be written as

$$f(x,y,z,t) = \omega t - k\left[l + \frac{r^2}{2l(1+z_R^2/l^2)}\right] + \arctan(l/z_R), \tag{9}$$

where

$$l^2 = x^2\sin^2\theta + (y+ut)^2\cos^2\theta + x(y+ut)\sin 2\theta - z^2, \tag{10}$$

and

$$r^2 = \left[x\cos\theta + (y+ut)\sin\theta\right]^2 + z^2. \tag{11}$$

Substituting Eqs. (10) and (11) into Eq. (9) and subsequently into Eq. (8), it becomes clear that it becomes possible for zeroes in the vector potential to propagate through the plasma for a short distance independent of the angle of polarisation.

Having established that there are zeroes in the vector potential propagating through the plasma, it is now prudent to discuss the behaviour of the electrons during the $\vec{A} = 0$ phase. By writing out the relativistic invariant of the momentum four-vector, one can obtain an expression for the Lorentz gamma factor of the fast electrons

$$\gamma^2 = 1 + \left(\frac{|\vec{p}|}{mc}\right)^2. \tag{12}$$

By applying the conservation of momentum to obtain $p_{\text{pol}} = a_0 mc$, and by assuming that the majority of the momentum from the boring effect of the laser pulse goes into the direction of propagation such that $p_{\text{prop}} \gg p_\perp$, it is possible to obtain an expression for the speed of the electrons

$$v = \left[\frac{a_0^2 + (p_{\text{prop}}/mc)^2}{1 + a_0^2 + (p_{\text{prop}}/mc)^2}\right]^{1/2} c. \tag{13}$$

In the $\vec{A} = 0$ phase, Eq. (13) becomes

$$v_{\text{prop}} = \frac{1}{\sqrt{1 + (mc/p_{\text{prop}})^2}} c. \tag{14}$$

As the vector potential passes through zero, the electrons in the plasma reach up to the speed given in Eq. (14) and cross the region of positive space charge mentioned in Sec. II. This, in effect, is analogous to the electrons crossing a pseudo-capacitor system and gaining energy. These bunches are eventually launched back into the plasma with high momenta when the laser pulse reaches the peak amplitude again. The coherent and relativistic nature of the motion of these bunches led Baeva *et al*. to posit that there is an intrinsic link between the fast electrons created by the ZVP mechanism and the coherent x-rays seen in the high-order harmonic generation (HHG).[9] These coherent x-rays are characterised by their scaling of intensity with the harmonic order, q, which is predicted by theory,[11,26] and has been validated by experiments to be[27,28]

$$I(\omega_q) \sim \left(\frac{\omega_q}{\omega_0}\right)^{-8/3} \equiv q^{-8/3}, \tag{15}$$

where ω_0 is the fundamental frequency of the incident pulse and $\omega_q = q\omega$ is the frequency of the qth harmonic.

Thus, the two key signatures of the ZVP mechanism are coherent fast electron bunches co-propagating with zeroes in the vector potential, and an increased efficiency in HHG when zeroes in the vector potential are present.

IV. SCALING RELATIONS

In order to characterise the ZVP absorption mechanism and confirm the validity of the theory, it is necessary to consider how varying the parameters at play will impact upon the degree of absorption. The simplest, and the most intuitive, checks to make are how the kinetic energy of a single electron acted upon by this mechanism, and subsequently the electron fluid, scales with the initial conditions of the system. Note that this model does not apply to the bulk body of the electrons in the plasma but only to the fraction of the electrons that co-propagates with the zeroes in the vector potential.

If you consider displacing an electron fluid by a small vector $\Delta\vec{r}$, then a space charge of ions, Q, is left behind, given by

$$Q = en_e|\Delta\vec{r}|\sigma, \tag{16}$$

where n_e is the electron fluid number density, and σ is the cross-section that describes the space swept out by the electron fluid as it is displaced by $\Delta\vec{r}$.

During the adiabatic phase of the ZVP mechanism, the electrostatic force caused by the setup of this space charge, Q, is exactly compensated by the radiation pressure being exerted on the electrons by the laser pulse

$$P_E = P_L, \tag{17}$$

where P_E is the pressure due to the electrostatic force from the space charge, and P_L is the radiation pressure from the laser pulse. P_L is given by

$$P_L = \frac{1}{2}\epsilon_0 E_L^2 = \frac{\epsilon_0(a_0\omega_0 m_e c/e)^2}{2}, \tag{18}$$

where E_L is the electric field of the laser pulse, a_0 is the normalised intensity of the pulse, and ω_0 is the frequency of the pulse.

The pressure arising due to the space charge is given by

$$P_E = |Q\vec{E}_s|/\sigma, \tag{19}$$

where $\vec{E_s}$ is given by Gauss' law

$$\iint_S \vec{E_s} \cdot d\vec{\sigma} = Q/\epsilon_0. \tag{20}$$

This leads to an expression for the electrostatic pressure

$$P_E = (en_e|\Delta\vec{r}|)^2/\epsilon_0. \tag{21}$$

By substituting Eqs. (4), (18), and (21) into Eq. (17); an expression for $\Delta\vec{r}$ can be obtained

$$|\Delta\vec{r}| = \frac{\sqrt{2}}{4\pi}\frac{a_0 n_c}{n_e}\lambda = \frac{\sqrt{2}}{4\pi}\frac{\lambda}{S}. \tag{22}$$

From Eq. (22), it is easy to calculate the kinetic energy gain, T, of a single electron that crosses the pseudo-capacitor of the electric field $\vec{E} = en_e\Delta\vec{r}/\epsilon_0$, and therefore, the total kinetic energy of the electron fluid, U

$$T = e\vec{E}\cdot\Delta\vec{r} \propto \frac{a_0^2}{n_e\lambda^2}, \tag{23}$$

$$U = n_e\sigma|\Delta\vec{r}|T \propto \frac{a_0^3}{n_e\lambda^3}. \tag{24}$$

These scaling relations agree in form precisely with the previous one dimensional work done by Baeva *et al.*[9] They are easily reduced into two dimensions with an identical power law dependence on a_0, n_e, and λ recovered by using the two dimensional equivalents of Eq. (21)

$$P_E^{2D} = |Q\vec{E_S}|/L \tag{25}$$

(where L is the length of the boundary which the force lines cross, and $\hat{L}$ is the unit vector perpendicular to said boundary) and Eq. (20)

$$\oint_L \vec{E_S}\cdot d\vec{L} = Q/\epsilon_0^{2D}, \tag{26}$$

where ϵ_0^{2D} is the permittivity of free space with units adjusted to be consistent with a two-dimensional system. This indicates that even with the 2D PIC simulations, it should be possible to extract the correct scaling relations from the results.

V. PARTICLE-IN-CELL SIMULATIONS

Numerical simulations investigating the ZVP mechanism should be able to reproduce the core facets of the theory. These include the existence of zeroes in the vector potential moving through the plasma, fast electron bunches co-propagating with said zeroes, energy scalings obeying Eqs. (23) and (24), and a significant contribution from the ZVP mechanism to the intensity of coherent x-rays produced during the laser-plasma interaction. Such simulations were successfully conducted in one dimension by Baeva *et al.*[9] However, at higher dimensions, a number of instabilities, such as the hosing instability,[6,29–32] take effect. It is therefore desirable to check that the ZVP mechanism can still be observed in a system more vulnerable to instability.

The simulations described later were carried out using OSIRIS, a fully relativistic PIC code, in 2D[33] (i.e., two dimensional spatially but three dimensional in terms of velocity and field space). The grid for the simulation was set to be a square of side length $250k_0^{-1}$, where k_0 is the wavenumber of the incident laser pulse with 64 cells per k_0^{-1} in the $\hat{x}$-direction and 32 cells per k_0^{-1} in the $\hat{y}$-direction. This was sufficient to resolve the high momentum features in the electron profiles in Sec. V A, but the simulations at a higher resolution of 250 cells per k_0^{-1} in each direction were performed to resolve the coherently generated x-rays described in Sec. V D.

The plasma targets were simulated using the 16 electron macro-particles and 4 ion macro-particles per cell with the mass-to-charge ratio of the ions being set at 3660 times larger than that of the electrons. The targets were modelled as parabolic plasma mirrors[34,35] with a radius of curvature of $500k_0^{-1}$. This target shape was chosen as it was found that the x-rays generated from a rectangular target were significantly more divergent making the intensity spectrum of the generated radiation more difficult to extract. The front of the target (as can be seen in Fig. 2) was characterised with an exponentially decaying profile in the radial direction of the mirror, with a scale length of $0.4k_0^{-1}$. This was done to ensure the efficient generation of coherent x-rays from the targets while maintaining a sharp density gradient.[36–38] The density of the main body of the plasma mirror was varied from $n_e = 25n_c$ to $n_e = 100n_c$.

The laser pulse was simulated as a p-polarised Gaussian pulse to ensure that the momenta in the direction of the polarisation could be faithfully extracted. The pulse duration was set to $160\omega_0^{-1}$, where ω_0 is the frequency of the pulse, which was focused down to a spot diameter of $12\pi k_0^{-1}$. The normalised vector potential of the pulse was varied from $a_0 = 5$ to $a_0 = 100$ over the course of the simulations and included one run where a circularly polarised pulse was used to investigate the case of a vector potential that never passes through zero.

A. High-momentum spikes

To qualitatively provide evidence of the existence of the ZVP mechanism, the laser pulse was set incident on the plasma in the $\hat{x}$-direction and the phase-space plots

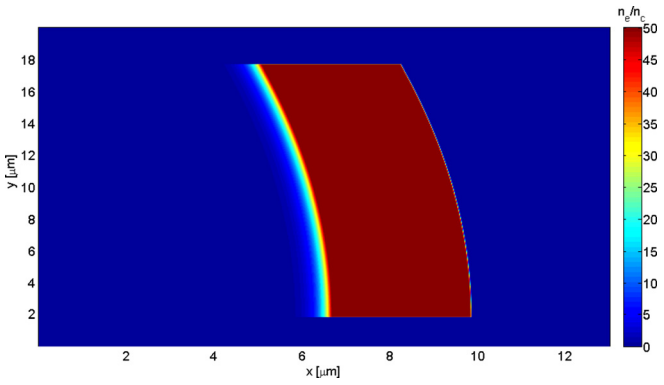

FIG. 2. Typical initial target profile, in this case with the bulk of the plasma mirror being characterised by $n_e/n_c = 100$.

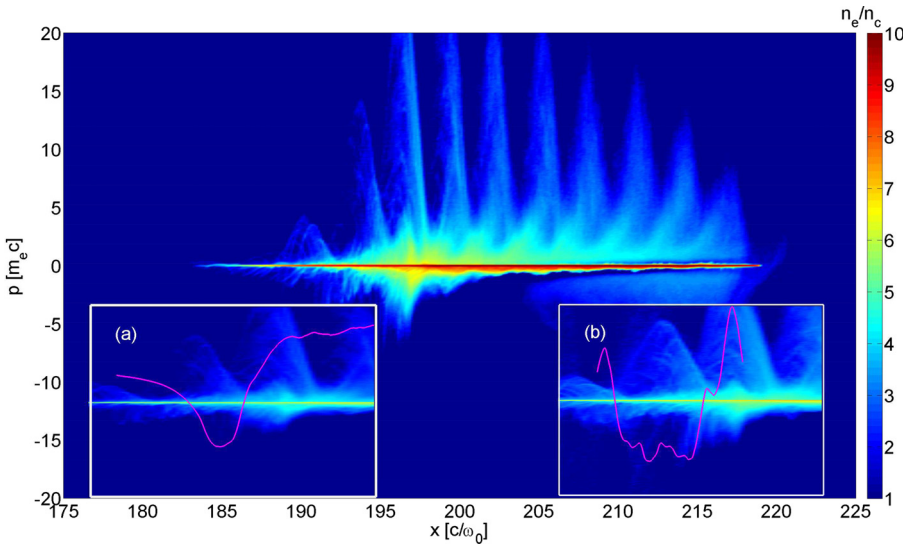

FIG. 3. A $p_x - x$ phase space plot for the case of $a_0 = 30$, $n_e = 50 n_c$ with the transverse vector potential of the system overlaid in insets (a) and (b) showing the onset of the co-propagating electron bunches that are characteristic of the ZVP mechanism with the time step in (a) being a zoom of the main figure and taking place 1/5th of a wave cycle before the time step in (b).

displaying the electron charge distribution on a $p_x - x$ phase diagram were extracted from the results.

Figure 3 shows such a phase diagram with the two insets displaying first the vector potential, A, overlaid on the phase space in frames separated by approximately 1/5th of a wave cycle in time where in each case the vector potential has been calculated by taking the current density outputs, $\vec{J}$ of the simulation and integrating them as in Eq. (1) to yield $\vec{A}$. It can be seen from the first inset (corresponding to the same time frame as the bulk of the figure) that the location of the emergence of the high momentum spikes coincides with the position at which the vector potential passes through zero. In the second inset—corresponding to a later time—it is evident that the momentum spikes have moved along with the pulse. This provides the first evidence, albeit qualitative, that the ZVP mechanism is at work in this regime.

A further check to ensure that the high-momentum spikes can genuinely be attributed to the ZVP mechanism is to verify that the high longitudinal momenta of the electrons are only observed for pulses where the vector potential passes through zero. This was done by conducting the same test as previously described but instead using a pulse with circular polarisation as opposed to linear. The resulting $p_x - x$ phase space is shown in Fig. 4. Not only are the highest longitudinal momenta much lower for the circularly polarised case, it is also immediately obvious that—as expected—the lack of zeroes in the vector potential has removed the high momentum bunches, which penetrate the plasma in the linearly polarised case.

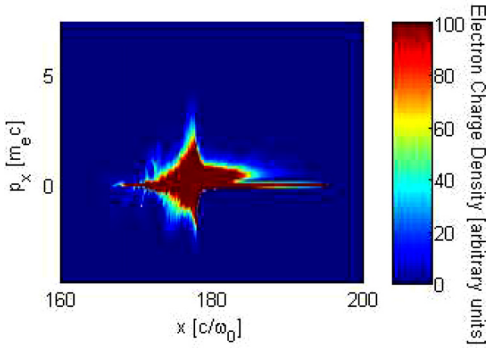

FIG. 4. $p_x - x$ phase space plot for the case of a circularly polarised pulse. Clearly, there are no high longitudinal momenta spikes.

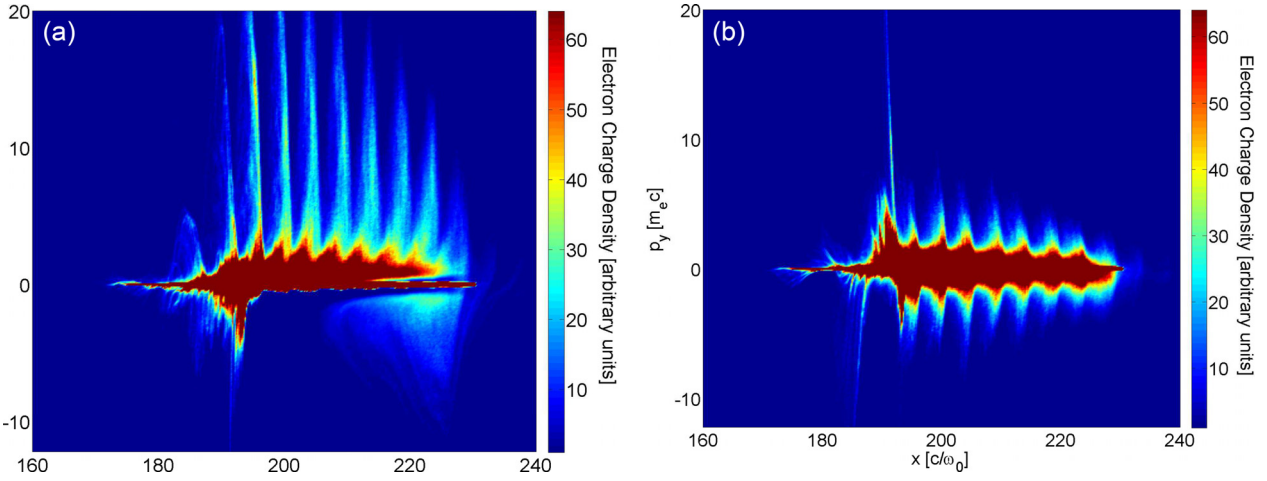

FIG. 5. $p_x - x$ (a) and $p_y - x$ (b) phase spaces for an obliquely incident pulse. The high momentum bunches are seen to be propagating in the direction of the incident laser pulse and with no discernible high momentum electrons transverse to the beam.

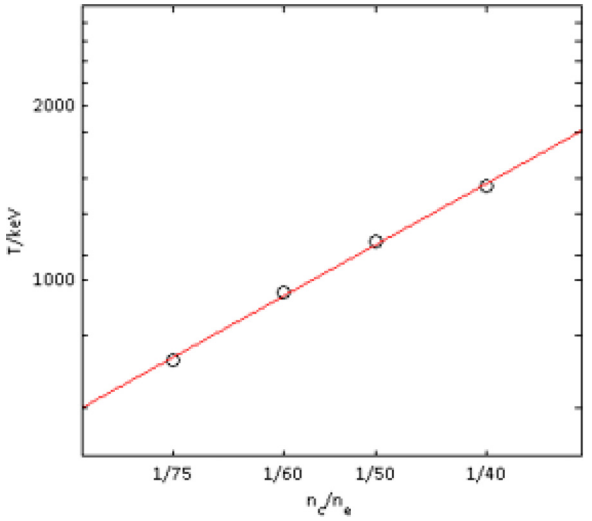

FIG. 6. Log-log plot of the $1/n_e$ dependence of the fast electron energy. Plotted points indicate energies extracted from 2D PIC simulations for the case $a_0 = 30$ for a range of densities, with a fit to the points yielding a gradient of 1.11 ± 0.04.

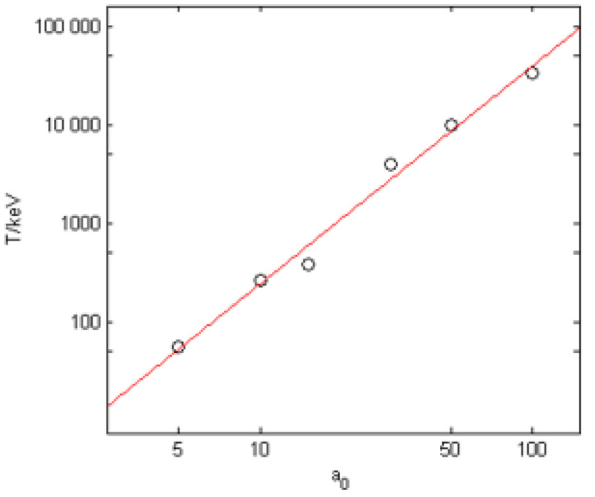

FIG. 7. Log-log plot of the a_0^2 dependence of the fast electron energy (fast meaning electrons in the high-momentum bunches only). Plotted points indicate energies extracted from 2D PIC simulations for the case $n_e = 50n_c$ for a range of normalised vector potential values, with a fit to the points yielding a gradient of 2.15 ± 0.17.

B. Oblique incidence

To investigate the extent to which the oblique incidence affects the launching of the fast electrons into the plasma, the target was rotated such that there was an angle of 30° between the normal of the plasma's ablating surface and the laser pulse propagating in the $\hat{x}$-direction. $p_x - x$ and $p_y - x$ phase spaces were then extracted, as seen in Fig. 5. It is clear that despite the re-orientation of the target, the high momentum bunches are still co-propagating with the pulse along the $\hat{x}$ direction with no identifiable high momentum features in the direction transverse to the beam. This validates the prediction of the ZVP theory that the electron bunches are launched into the plasma longitudinally with respect to the pulse and independent of the relative orientation between the plasma and the incident beam.

C. Scaling relations

To check the validity of Eqs. (23) and (24) the kinetic energy of the electrons in the high momentum spikes (as shown in Fig. 3) was extracted at the same time-step for several simulations. These simulations were divided into two sets. The first set varied the plasma density for a constant value of $a_0 = 30$, whilst the second varied a_0 for a constant value of $n_e = 50n_c$.

Figure 6 shows that the inverse linear dependence of the fast electron kinetic energy with n_e is in a very good agreement with Eq. (23). The simulations extract a dependence of energy on the density of $T \sim n_e^{-1.11 \pm 0.04}$, matching closely with the predicted dependence of $T \sim n_e^{-1}$ in Eq. (23). Similarly, Fig. 7 shows a dependence of the electron kinetic energy on the vector potential; in these simulations, a power

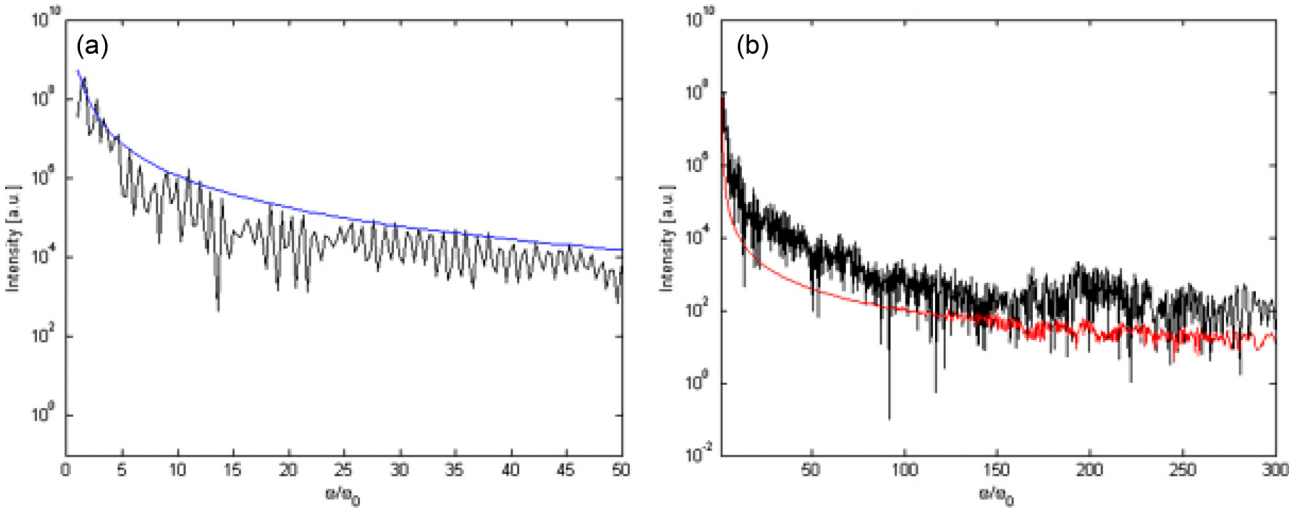

FIG. 8. (a) Intensity spectra of the coherent x-rays reflected from the simulation target in the linearly polarised case with the power law given in Eq. (15) fitted (blue), demonstrating that the radiation produced over ZVP absorption matches the expected HHG spectrum with individual harmonics easily seen at least to the 50th order. (b) A comparison of the coherent x-ray spectrum for the linearly polarised (black) and circularly polarised (red) cases with the power law fit (blue) all extended to the 300th harmonic. The lack of coherent fast bunches of electrons in the circularly polarised case reduces the intensity of the coherent x-rays by almost two orders of magnitude.

law of $T \sim a_0^{2.15\pm0.17}$ is retrieved, in excellent agreement with the exponent of 2 predicted in Eq. (23).

D. Coherent x-ray generation

The final prediction of the ZVP mechanism to be tested relates to its contribution to HHG. In these simulations, an electron density of $n_e = 50n_c$ and a laser intensity of $a_0 = 30$ was used. The Fourier transform of the radiation reflected from the "plasma mirror"[34,35] was taken, and the spectrum is shown in Fig. 8. The form of the spectrum is seen to agree well with the power law predicted in Eq. (15). In contrast, the spectrum obtained using a circularly polarised pulse is found to be orders of magnitude less intense than in the linearly polarised case. This further validates the prediction that the ZVP mechanism is a significant contributor to HHG.

VI. CONCLUSIONS

In this paper, we have shown that the zero vector potential absorption mechanism posited by Baeva *et al.*, and previously given only a one dimensional exposition, can be described perfectly well in three dimensions. It has also been shown that this absorption mechanism is constrained to the plane containing the directions of polarisation and propagation of the vector potential of the incident pulse. The effect of this absorption is to produce attosecond-scale coherent fast electron bunches and x-rays. Numerical simulations in two dimensions faithfully reproduced the key predictions of the theory and agreed well with the physically motivated scaling relations derived in Sec. IV. The results of this work give further support to the ZVP concept through both qualitative and quantitative validation of its key predictions. In the future, we hope to investigate the potential applications of such short duration fast electron bunches and the coherent x-rays generated by them.

ACKNOWLEDGMENTS

Funding for this work was provided by the Science and Technology Facilities Council of the United Kingdom and EPSRC under Grant Nos. ST/P000967/1 and EP/N509711/1. A.S. acknowledges support from RCUK under student number 1796896. The authors are grateful for computing resources provided by STFC Computing Department's SCARF cluster and to the OSIRIS Consortium for access to the OSIRIS PIC code. A.S. is particularly grateful for the support of the staff at the Central Laser Facility without which none of this work would have been possible.

[1]G. A. Mourou, C. L. Labaune, M. Dunne, N. Naumova, and V. T. Tikhonchuk, "Relativistic laser-matter interaction: From attosecond pulse generation to fast ignition," Plasma Phys. Controlled Fusion **49**, B667 (2007).
[2]J. P. Zou, C. LeBlanc, D. N. Papadopoulos, G. Chériaux, P. Georges, G. Mennerat, F. Druon, L. Lecherbourg, A. Pellegrina, P. Ramirez, F. Giambruno, A. Fr'eneaux, G. Leconte, D. Badarau, J. M. Boudenne, D. Fournet, T. Valloton, J. L. Paillard, J. L. Veray, M. Pina, P. Monot, J. P. Chambaret, P. Martin, F. Mathieu, P. Audebert, and F. Amiranoff, "Design and current progress of the Apollon 10 PW project," High Power Laser Sci. Eng. **3**, e2 (2015).
[3]A. R. Bell and J. G. Kirk, "Possibility of prolific pair production with high-power lasers," Phys. Rev. Lett. **101**, 200403 (2008).
[4]S. F. Martins, J. Vieira, F. Fiuza, R. A. fonseca, C. Huang, W. Lu, W. B. Mori, R. Trines, P. Norreys, and L. O. Silva, "Numerical simulations of LWFA for the next generation of laser systems," Adv. Accel. Concepts **1086**, 285 (2009).
[5]A. P. L. Robinson, M. Zepf, S. Kar, R. G. Evans, and C. Bellei, "Radiation pressure acceleration of thing foils with circularly polarized laser pulses," New J. Phys. **10**, 013021 (2008).
[6]L. Ceurvorst, N. Ratan, M. C. Levy, M. F. Kasim, J. Sadler, R. H. H. Scott, R. M. G. M. Trines, T. W. Huang, M. Skramic, M. Vranic, L. O. Silva, and P. A. Norreys, "Mitigating the hosing instability in relativistic laser-plasma interactions," New J. Phys. **18**, 053023 (2016).
[7]N. Naumova, T. Schlegel, V. T. Tikhonchuk, C. Labaune, I. V. Sokolov, and G. Mourou, "Hole boring in a DT pellet and fast-ion ignition with ultraintense laser pulses," Phys. Rev. Lett. **102**, 025002 (2009).
[8]S. Gordienko, A. Pukhov, O. Shorokhov, T. Baeva, and T. Gordienko, "Coherent focusing of high harmonics: A new way towards the extreme intensities," Phys. Rev. Lett. **94**, 103903 (2005).
[9]T. Baeva, S. Gordienko, A. P. L. Robinson, and P. A. Norreys, "The zero vector potential mechanism of attosecond absorption," Phys. Plasmas **18**, 056702 (2011).
[10]J. D. Jackson, *Classical Electrodynamics* (John Wiley & Sons, 1975).
[11]U. Teubner and P. Gibbon, "High-order harmonics from laser-irradiated plasma surfaces," Rev. Mod. Phys. **81**, 445 (2005).
[12]J. Sadler, R. Nathvani, P. Oleśkiewicz, L. Ceurvorst, N. Ratan, M. F. Kasim, R. M. G. M. Trines, R. Bingham, and P. A. Norreys, "Compression of X-ray free electron laser pulses to attosecond duration," Sci. Rep. **5**, 16755 (2015).
[13]R. Neutze, R. Wouts, D. Van der Spoel, E. Weckert, and J. Hajdu, "Potential for biomolecular imaging with femtosecond X-ray pulses," Nature **406**, 752 (2000).
[14]F. Krausz and M. Ivanov, "Attosecond physics," Rev. Mod. Phys. **81**, 163 (2009).
[15]J. Li, X. Ren, Y. Yin, K. Zhao, A. Chew, Y. Cheng, E. Cunningham, Y. Wang, S. Hu, Y. Wu, M. Chini, and Z. Chang, "53-attosecond X-ray pulses reach the carbon K-edge," Nat. Commun. **8**, 186 (2017).
[16]S. C. Wilks, W. L. Kruer, M. Tabak, and A. B. Langdon, "Absorption of ultra-intense laser pulses," Phys. Rev. Lett. **69**, 1383 (1992).
[17]S. C. Wilks and W. L. Kruer, "Absorption of utrashort, ultra-intense laser light by solids and overdense plasmas," IEEE J Quantum Electron. **33**, 1954 (1997).
[18]F. Brunel, "Not-so-resonant, resonant absorption," Phys. Rev. Lett. **59**, 52 (1987).
[19]W. Forslund, J. M. Kindel, and K. Lee, "Theory of hot electron spectra at high laser intensity," Phys. Rev. Lett. **39**, 284 (1977).
[20]P. Mulser, D. Bauer, and H. Ruhl, "Collisionless laser-energy conversion by anharmonic resonance," Phys. Rev. Lett. **101**, 225002 (2008).
[21]P. Gibbon and A. R. Bell, "Collisionless absorption in sharp-edged plasmas," Phys. Rev. Lett. **68**, 1535 (1992).
[22]S. Gordienko and A. Pukhov, "Scalings for ultrarelativistic laser plasmas and quasimonoenergetic electrons," Phys. Plasmas **12**, 043109 (2005).
[23]F. F. Chen, *Introduction to Plasma Physics and Controlled Fusion Volume 1: Plasma Physics* (Plenum Press, United States of America, 1984).
[24]A. M. Steane, *Relativity Made Relatively Easy* (OUP, United Kingdom, 2012).
[25]C. C. Davis, *Lasers and Electro-Optics - Fundamentals and Engineering* (Cambridge University Press, 1996).
[26]T. Baeva, S. Gordienko, and A. Pukhov, "Theory of high-order harmonic generation in relativistic laser interaction with over-dense plasma," Phys. Rev. E **74**, 046404 (2006).
[27]B. Dromey, M. Zepf, A. Gopal, K. Lancaster, M. S. Wei, K. Krushelnick, M. Tatarakis, N. Vakakis, S. Moutaizis, R. Kodama, M. Tampo, C. Stoeckl, R. Clarke, H. Habara, D. Neely, S. Karsch, and P. A. Norreys, "High harmonic generation in the relativistic limit," Nat. Phys. **2**, 456 (2006).
[28]B. Dromey, S. Kar, C. Bellei, D. C. Carroll, R. J. Clarke, J. S. Green, S. Kneip, K. Markey, S. R. Nagel, P. T. Simpson, L. Willingale, P. McKenna, D. Neely, Z. Najmudin, K. Krushelnick, P. A. Norreys, and M. Zepf, "Bright multi-keV harmonic generation from relativistically oscillating plasma surfaces," Phys. Rev. Lett. **99**, 115003 (2007).
[29]G. Li, R. Yan, and C. Ren, "Laser channeling in millimeter-scale underdense plasmas of fast-ignition targets," Phys. Rev. Lett. **100**, 125002 (2008).
[30]G. Sarri, K. L. Lancaster, R. Trines, E. L. Clark, S. Hassan, J. Jiang, N. Kageiwa, N. Lopes, R. Ramis, A. Rehman, X. Ribeyre, C. Russo, R. H. H.

Scott, T. Tanimoto, M. Temporal, M. Borghesi, J. R. Davies, Z. Najmudin, K. A. Tanaka, M. Tatarakis, and P. A. Norreys, "Creation of persistent, straight, 2 mm long laser driven channels in underdense plasmas," Phys. Plasmas **17**, 113303 (2010).
[31]Z. Najmudin, K. Krushelnick, M. Tatarakis, E. L. Clark, C. N. Danson, V. Malka, D. Neely, M. I. K. Santala, and A. E. Dangor, "The effect of high intensity laser propagation instabilities on channel formation in underdense plasmas," Phys. Plasmas **10**, 438 (2003).
[32]L. M. Chen, H. Kotaki, K. Nakajima, J. Koga, S. V. Bulanov, T. Tajima, Y. Q. Gu, H. S. Peng, X. X. Wang, T. S. Wen, H. J. Liu, C. Y. Jiao, C. G. Zhang, X. J. Huang, Y. Guo, K. N. Zhou, J. F. Hua, W. M. An, C. X. Tang, and Y. Z. Lin, "Self-guiding of 100 TW femtosecond laser pulses in centimeter-scale underdense plasma," Phys. Plasmas **14**, 040703 (2007).
[33]R. A. Fonseca, L. O. Silva, F. S. Tsung, V. K. Decyk, W. Lu, C. Ren, W. B. Mori, S. Den, S. Lee, T. Katsouleas, and J. C. Adam, "OSIRIS: A three-dimensional, fully relativistic particle in cell code for modelling plasma based accelerators," Lect. Notes. Comput. Sci. **2231**, 342 (2002).
[34]C. Thaury, F. Quéré, J.-P. Geindre, A. Levy, T. Ceccotti, P. Monot, M. Bougeard, F. Réau, P. D'Oliveira, P. Audebert, R. Marjoribanks, and P. Martin, "Plasma mirrors for ultrahigh-intensity optics," Nat. Phys. **3**, 424 (2007).
[35]H. Vincenti, S. Monchocé, S. Kahaly, G. Bonnaud, P. Martin, and F. Quéré, "Optical properties of relativistic plasma mirrors," Nat. Commun. **5**, 3403 (2014).
[36]F. Dollar, P. Cummings, V. Chvykov, L. Willingale, M. Vargas, V. Yanovksy, C. Zulick, A. Maksimchuk, A. G. R. Thomas, and K. Krushelnick, "Scaling high-order harmonic generation from laser-solid interactions to ultrahigh intensity," Phys. Rev. Lett. **110**, 175002 (2013).
[37]M. Zepf, G. D. Tsakiris, G. Pretzler, I. Watts, D. M. Chambers, P. A. Norreys, U. Andiel, A. E. Dangor, K. Eidmann, C. Gahn, A. Machacek, J. S. Wark, and K. Witte, "Role of the plasma scale length in the harmonic generation from solid targets," Phys. Rev. E **58**, R5253 (1998).
[38]A. Tarasevitch, A. Orisch, D. Von Der Linde, P. Balcou, G. Rey, J.-P. Chambaret, U. Teubner, D. Klöpfel, and W. Theobald, "Generation of high-order spatially coherent harmonics from solid targets by femtosecond laser pulses!," Phys. Rev. A **62**, 1 (2000).